EXPERIMENTAL VALIDATION OF A MODEL FOR LIQUID LEVELS AND HEAT TRANSFER RATES IN A CLOSED TWO-PHASE THERMOSYPHON

C. Petroff
Department of Mechanical Engineering
Massachusetts Institute of Technology
Cambridge, Massachusetts

G. P. Beretta
Department of Mechanical Engineering
Massachusetts Institute of Technology
Cambridge, Massachusetts
and Dipartimento di Ingegneria Meccanica
Universita di Brescia
Brescia, Italy

HTD-Vol. 104

VOLUME THREE

Buoyant Plumes in the Environment
Future Challenges in Environmental Heat Transfer
Measurements of Tissue Heat Transfer
Heat Transfer for Manufacturing in Space
General Papers

COLLECTED PAPERS IN HEAT TRANSFER 1988

presented at
THE WINTER ANNUAL MEETING OF
THE AMERICAN SOCIETY OF MECHANICAL ENGINEERS
CHICAGO, ILLINOIS
NOVEMBER 27-DECEMBER 2, 1988

sponsored by
THE HEAT TRANSFER DIVISION

edited by
K. T. YANG
UNIVERSITY OF NOTRE DAME

THE AMERICAN SOCIETY OF MECHANICAL ENGINEERS
United Engineering Center 345 East 47th Street New York, N.Y. 10017

EXPERIMENTAL VALIDATION OF A MODEL FOR LIQUID LEVELS AND HEAT TRANSFER RATES IN A CLOSED TWO-PHASE THERMOSYPHON

C. Petroff
Department of Mechanical Engineering
Massachusetts Institute of Technology
Cambridge, Massachusetts

G. P. Beretta
Department of Mechanical Engineering
Massachusetts Institute of Technology
Cambridge, Massachusetts
and Dipartimento di Ingegneria Meccanica
Universita di Brescia
Brescia, Italy

ABSTRACT

A method for the determination of steady-state liquid levels and heat transfer rates in a closed two-phase thermosyphon is presented and validated with experimental data from a copper thermosyphon with water as the working fluid, fluid inventory ranging from 25 % to 150 % of the evaporator volume, operating fluid temperatures ranging from 20°C to 120°C, and inclination 45° and vertical. In addition, the use of an internal downcomer is shown to increase the operating limit by 300 %.

INTRODUCTION

Closed two-phase thermosyphons have been successfully commercialized in home and industrial gas burners for space heating. Among the factors that determine the operating limits of a thermosyphon is the fluid inventory, i.e., the amount of working fluid with which the thermosyphon is filled.

The present experimental study investigates the role of liquid level on the performance of the thermosyphon. The average steady-state liquid level and the heat-transfer rates can be estimated using a model based on the "drift-flux" model of two-phase flow. At high fluid inventories and high power throughput, part of the liquid is found to remain blocked permanently at the top of the thermosyphon thus reducing the area available for condensation and, hence, the overall effective conductivity of the device. This effect can be circumvented by guaranteeing the liquid return through an internal downcomer.

EXPERIMENTAL APPARATUS

A schematic diagram of the experimental apparatus used in this study is shown in Figure 1. The copper thermosyphon has inside diameter D = 14 mm, wall thickness 3 mm, and thermocouples laid flat in slots milled into the wall from outside. The evaporator is heated by electric cartridge heaters, and the condenser is cooled by a water jacket. The adiabatic section consists of a glass tube attached to the copper tube by "O"-rings. Both ends of the thermosyphon are sealed by removable end caps, and thermocouples are inserted through each end cap to measure centerline fluid temperatures in the evaporator and condenser sections. The upper thermocouple can be replaced by a glass window to allow flow visualization.

The steady-state power throughput in the thermosyphon is determined from the temperature-rise measurement from RTD's placed at the inlet and outlet sections of the water jacket, and the flow-rate measurement from a turbine flowmeter in the cooling circuit. The resulting data are in good agreement with estimates of the power throughput based on the electric power supplied to the heaters.

EXPERIMENTAL PROCEDURE

To remove dissolved gases, the working fluid is first boiled for several minutes and then poured into the top of the thermosyphon. The condenser end cap is closed and vacuum is drawn. To verify that non-condensible gases do not affect the heat transfer rates, some vapor is vacuumed off during operation through the valve at the top, and the measured overall heat transfer coefficients are checked to remain unaffected.

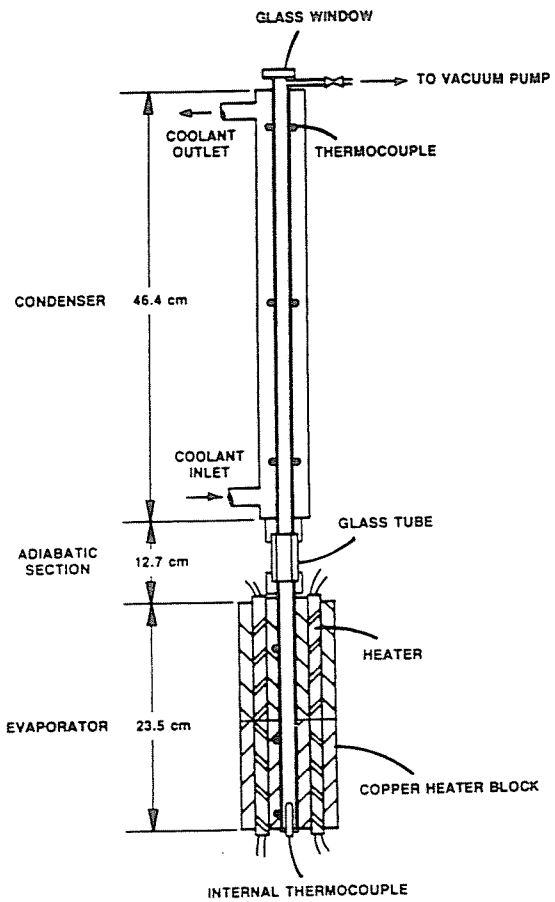

Figure 1. Sketch of the experimental apparatus.

Data are taken with a quasi-steady approach. Operating conditions are changed slowly enough, compared with the thermal time constant of the thermosyphon, to ensure an almost steady-state operation. During a typical run, the coolant temperature is held constant at a prefixed value, while the electric-heater power is increased slowly until an operating limit is detected. Then, the coolant temperature is set at a higher value and the procedure repeated.

As power throughput is increased, the liquid level in the thermosyphon rises. A record is kept of the power throughput and the working fluid temperature above which the liquid level is observed to be steadily above the top of the glass midsection. The same is done for the values above which the liquid level intermittently reaches the top end cap, and for the values above which a layer of liquid permanently covers the top end cap, even between the intermittent rising of slugs.

DRIFT-FLUX MODEL FOR THE STEADY-STATE AVERAGE LIQUID LEVEL

Due to the vapor flow caused by boiling in the evaporator, the average liquid level under steady-state operation is higher than the zero-power liquid level. According to the flow-regime maps obtained by Shoham (Shoham, 1982), if the liquid inventory is enough to form a slug and the thermosyphon is vertical, then slug flow or churn flow occur under all operating conditions up to the flooding limit of operation. For these flow regimes, the average liquid level is the height at which the slugs break up because there is not enough liquid to form a bridge across them. Knowledge of the average liquid level is important for predicting the heat transfer performance of the thermosyphon as discussed below.

The drift-flux model developed by Wallis (Wallis, 1969) for two-phase flow can be adapted to the thermosyphon configuration because the dimensionless inverse viscosity

$$N_f = \frac{[D^3 g(\rho_f - \rho_g)\rho_f]^{1/2}}{\mu_f} \tag{1}$$

is greater than 300.

For a fully turbulent slug flow, the drift-flux model predicts a time averaged void fraction

$$\alpha = \frac{j_g}{1.2(j_f + j_g) + C_b v_{gj}} \tag{2}$$

where j_g and j_f are the vapor and liquid "superficial" velocities, v_{gj} the bubble drift velocity, and C_b an empirical number determined by Griffith (Griffith, 1964) to be 1.0 for unheated sections, and 1.6 for heated sections where boiling occurs.

For a vertical pipe, the bubble drift velocity

$$v_{gj} = K_1 \rho_f^{-1/2}[gD(\rho_f - \rho_g)]^{1/2} \tag{3}$$

where K_1 is a constant expressed in terms of the dimensionless inverse viscosity N_f and the Eötvos number $N_{eö} = D^2 g(\rho_f - \rho_g)/\sigma$,

$$K_1 = 0.345\,[1 - e^{(-N_f/34.5)}]\,[1 - e^{(3.37 - N_{eö})/10}] \tag{4}$$

In terms of the power throughput Q and the cross sectional area A_x the values of j_g and j_f in the adiabatic section are, respectively,

$$j_{ga} = \frac{Q}{h_{fg} A_x \rho_g} \tag{5}$$

$$j_{fa} = \frac{Q}{h_{fg} A_x \rho_f} \tag{6}$$

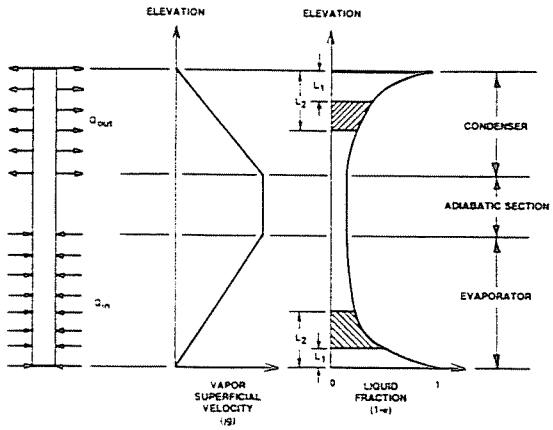

Figure 2. Sketch of superficial velocities and liquid fraction as a function of elevation in the thermosyphon.

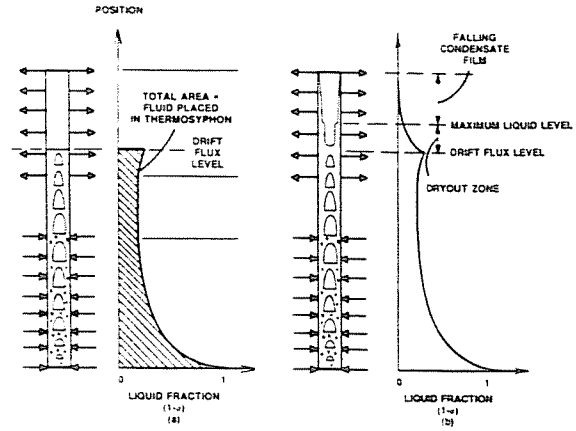

Figure 3. Sketch of the steady-state average liquid level in the thermosyphon.

Clearly, j_g and j_f range from zero at either end of the thermosyphon to their maximum value in the adiabatic section. Because $j_{fa} \ll j_{ga}$ it follows that $j_f \ll j_g$ anywhere in the thermosyphon. Equation 2 yields the liquid fraction

$$1 - \alpha = 1 - \frac{j_g}{1.2j_g + C_b v_{gj}} \tag{7}$$

In the evaporator, assuming that j_g varies linearly from 0 to j_{ga} as the distance L_x from the bottom end varies from 0 to L_e, yields $j_g = j_{ga}L_x/L_e$ (Figure 2). Thus, Equation 7 with $C_b = 1.6$ can be integrated between any two locations L_1 and L_2 (in the evaporator) to yield the volume $(V_{12})_e$ of liquid between L_1 and L_2

$$(V_{12})_e = A_x\left(\frac{L_2 - L_1}{6} + \frac{1.6v_{gj}L_e}{1.44j_{ga}} \ln \frac{1.6v_{gj} + 1.2L_2 j_{ga}/L_e}{1.6v_{gj} + 1.2L_1 j_{ga}/L_e}\right) \tag{9}$$

In the condenser, assuming that j_g varies linearly from 0 to j_{ga} as the distance L_x from the top end varies from 0 to L_c yields $j_g = j_{ga}L_x/L_c$ and Equation 7 with $C_b = 1.0$ can be integrated between any two locations L_1 and L_2 (in the condenser) to yield the volume $(V_{12})_c$ of liquid between L_1 and L_2, i.e.,

$$(V_{12})_c = A_x\left(\frac{L_2 - L_1}{6} + \frac{v_{gj}L_c}{1.44j_{ga}} \ln \frac{v_{gj} + 1.2L_2 j_{ga}/L_c}{v_{gj} + 1.2L_1 j_{ga}/L_c}\right) \tag{10}$$

In the adiabatic section, $j_g = j_{ga}$ and the volume of liquid between L_1 and L_2 is

$$(V_{12})_a = A_x(L_2 - L_1)\left(1 - \frac{j_{ga}}{1.2j_{ga} + v_{gj}}\right) \tag{11}$$

For a given power throughput Q and the resulting working fluid temperature, the time-averaged liquid level can be estimated as follows. First, the values of v_{gj} and j_{ga} are calculated. Then, the average liquid level is the level at which the sum of the volumes of liquid in the evaporator, adiabatic section and condenser are equal to the zero-power initial volume V_i (Figure 3). A more accurate estimate would also account for the volume V_{film} of the falling condensate that can be estimated using Nusselt's condensation theory (Rohsenow and Choi, 1961). The resulting average liquid level, the "drift-flux level" L_p, can be used to estimate heat rates as described below.

As discussed later (Figure 8), when the calculated drift-flux level is above the top of the thermosyphon, a plug of liquid is permanently sustained at the top of the condenser. The height of the liquid plug, called the blocked length, can be estimated from the analysis just described for the average liquid level, except that the vapor superficial velocity is assumed to decrease linearly from j_{ga} at the bottom of the condenser to zero at the bottom of the blocked length. Noncondensibles would collect above the liquid plug at the top of the thermosyphon.

EFFECT OF AVERAGE LIQUID LEVEL ON OVERALL HEAT TRANSFER COEFFICIENTS

In heat pipe practice, it is common to define overall heat transfer coefficients for the evaporator and the condenser based on the working fluid temperature (defined as the temperature in the adiabatic section) and the average temperatures of the evaporator and condenser walls, respectively.

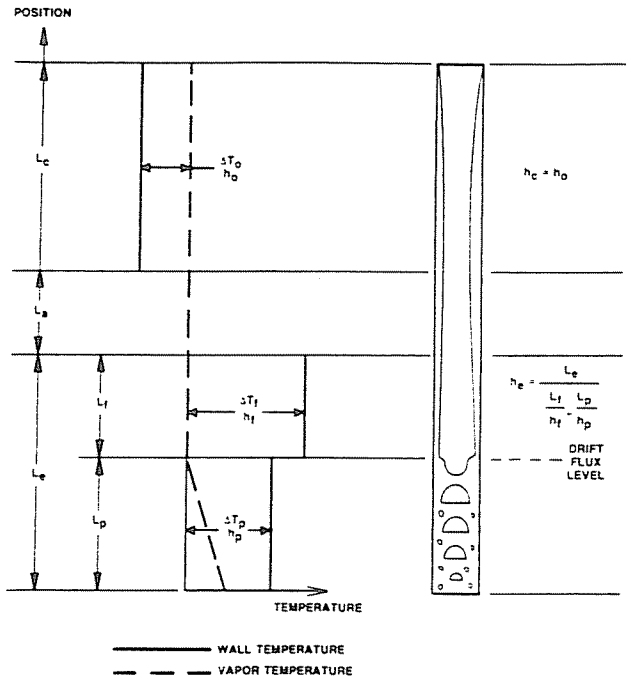

Figure 4. Schematic diagram showing the subdivision of the thermosyphon into regions with different heat transfer coefficients.

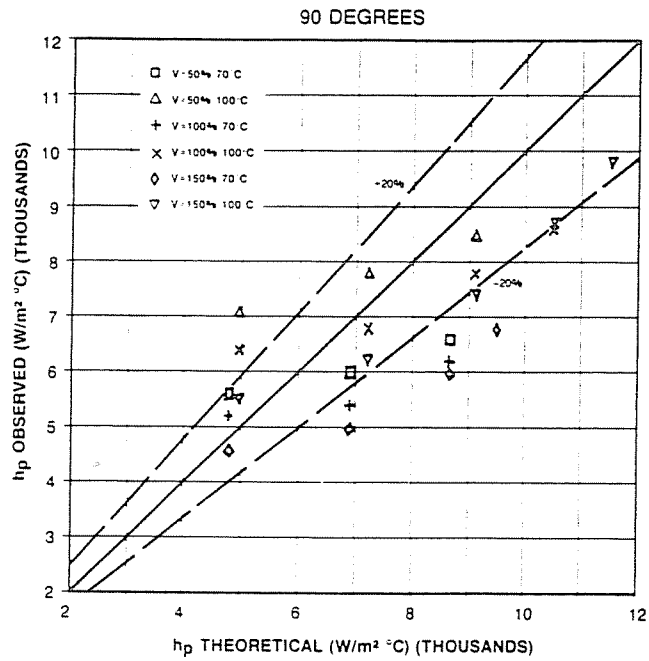

Figure 5. Comparison of estimated values of the evaporator overall heat transfer coefficient $h_e = h_p$ for $L_p > L_e$ versus measured values.

In this study, the temperature in the adiabatic section is not measured directly but estimated on the basis of the temperature measurements of the bottom and top thermocouples, and the results of a calibrating test for each fluid inventory (Petroff, 1988). The resulting experimental data on overall heat transfer coefficients are graphed in contour maps of h_e and h_c on a power-throughput versus working-fluid-temperature plane where the contour lines are smoothed by a fourth order polynomial least squares fit (Petroff, 1988).

When the average liquid level is in the evaporator, as sketched in Figure 4, the overall heat transfer coefficient can be broken into two parts corresponding to the evaporator area above and below the average liquid level

$$h_e = \frac{L_e}{L_f/h_f + L_p/h_p} \quad \text{for} \quad L_p < L_e \tag{12}$$

otherwise, $h_e = h_p$ for $L_p > L_e$. For the area below the average liquid level, the nucleate-boiling heat transfer coefficient can be estimated with the Shiraishi correlation (Shiraishi, Kikuchi and Yamanishi, 1982) which is based on the earlier Kusuda-Imura correlation (Kusuda and Imura, 1973),

$$h_p = 0.32 \frac{\rho_f^{0.65} k^{0.3} c_p^{0.7} g^{0.2}}{\rho_g^{0.25} h_{fg}^{0.4} \mu_f^{0.1}} \left(\frac{p}{p_a}\right)^{0.23} \left(\frac{Q}{A_e}\right)^{0.4} \tag{13}$$

For the area above the liquid level, the film-evaporation heat transfer coefficient can be estimated, assuming a countinuous film layer on the wall, with the Andros-Florschuetz correlation (Andros and Florsehuetz, 1978),

$$h_f = k \left(\frac{\rho_f^2 h_{fg} g}{\mu_f}\right)^{1/3} \left(\frac{3(L_p + L_f/2)Q}{A_e}\right)^{-1/3} \tag{14}$$

In Figures 5 and 6, the results of these estimates are compared with the measured values. For high average liquid levels (Figure 5, $L_p > L_e$, $h_e = h_p$), the data are in good agreement with those of Shiraishi, Kikuchi and Yamanishi (1982). For lower average liquid levels (Figure 6, $0.6L_e < L_p < L_e$), the agreement with the data is not as good because Equation 14 overestimates the film-evaporation heat transfer coefficient h_f. As also noticed by Cohen and Bayley (1955) and by Shiraishi, Kikuchi and Yamanishi (1982), the assumption of a continuous film layer overestimates the actual heat transfer coefficient because the film breaks down into rivulets and the uncovered areas are cooled much less effectively.

When the average liquid level does not reach into the condenser, the overall heat transfer coefficient in the condenser can be estimated using Nusselt's theory. For a vertical pipe, this yields

$$h_o = 0.925\, k \left(\frac{\rho_f(\rho_f - \rho_g) h_{fg} g}{\mu_f}\right)^{1/3} \left(\frac{Q}{A_x}\right)^{-1/3} \tag{15}$$

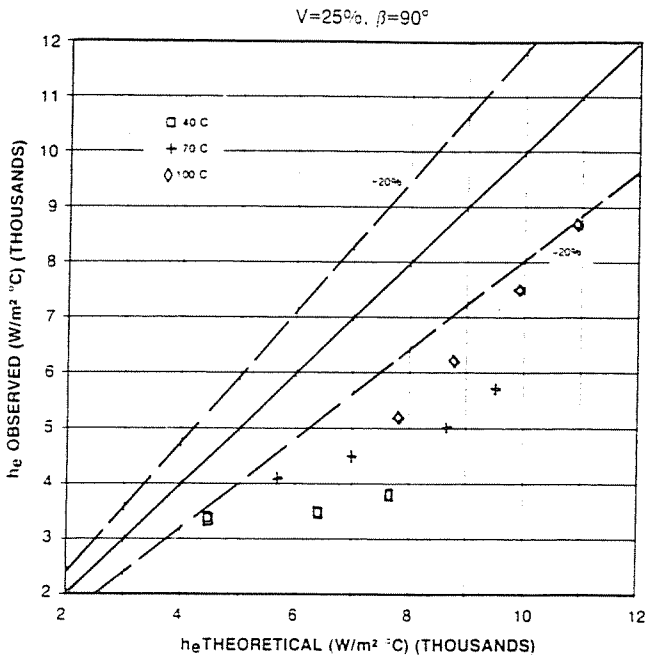

Figure 6. Comparison of estimated values of the evaporator overall heat transfer coefficient h_e for $0.6L_e < L_p < L_e$ versus measured values.

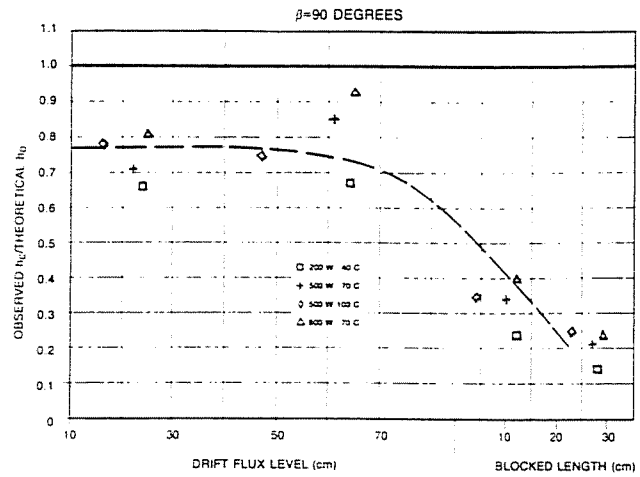

Figure 7. Measured values of the condenser overall heat transfer coefficient h_c (normalized by the Nusselt values) versus estimated average liquid level.

As the average liquid level increases into the condenser section, film condensation is replaced by condensing slug flow, for which no applicable correlation has been found. In principle, the overall heat transfer coefficient in the condenser can be broken into two parts corresponding to the condenser area above and below the average liquid level, as just done for the evaporator.

Experimental data for the condenser overall heat transfer coefficient are shown in Figure 7 as a function of calculated average liquid level (drift-flux level) and normalized by the Nusselt h_o. At low average liquid levels, the Nusselt theory overestimates the heat transfer coefficient by about 25%. At higher average liquid levels, the contribution of condensing slug-flow does not seem to degrade the heat transfer coefficient significantly.

Figure 7 shows that the condenser heat transfer coefficient is degraded significantly when the average liquid level reaches the top end of the thermosyphon and a blocked length is present. The reason for this effect is that the liquid plug reduces the effective area of the condenser and, hence, the performance of the thermosyphon.

AVERAGE LIQUID LEVELS AND LIQUID LEVEL FLUCTUATIONS

As the power throughput is slowly increased during the test procedure already described, the experimental apparatus allows to visualize the following three conditions concerning liquid levels: (a) the liquid level is steadily above the top of the glass midsection; (b) the liquid level reaches the top end cap intermittently; and (c) a layer of liquid covers the top end cap permanently.

Table 1 shows typical data on these observations, as well as estimates of the average liquid level L_p, the "vapor superficial velocity" j_g, the dryout-zone length L_h, the sum $L_p + L_h$, and the blocked length L_b, where the dryout zone is the region above the average liquid level where the rising slugs break up. The dryout-zone length is the difference between the maximum level reached by this intermittent breaking up of slugs and the calculated average liquid level or drift-flux level. At times, a rising of entrained droplets is observed, but this is not included in the dryout length.

For values of j_g up to 2.2 m/s, at the calculated average liquid level, the dryout-zone length L_h can be estimated with data obtained by Griffith, Mohamed and Brown (1988) and correlated by the relation

$$L_h = (0.14\ s)\ j_g \quad \text{for} \quad \alpha > 0.45 \qquad (16)$$

L_h is negligible for $\alpha < 0.45$. For $j_g > 2.2$ m/s no correlation is available. There is currently no method to calculate the liquid fraction in the dryout zone.

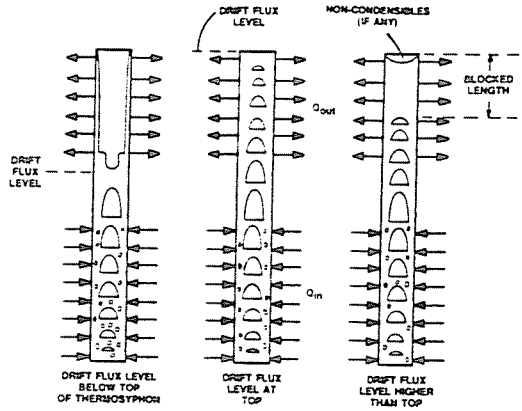

Figure 8. Sketch showing average liquid levels and the blocked length.

Table 1a. Observed liquid level reaches the top of the glass midsection (31.8 cm).

Operating point				Estimated values				
V_i/V_e %	β	Q W	T °C	L_p cm	j_g m/s	L_h cm	L_p+L_h cm	L_b cm
25	90°	550	27	29	60	-	-	-
25	90°	600	40	28	32	-	-	-
25	45°	550	32	28	46	-	-	-
25	45°	520	50	24	15	-	-	-
50	90°	200	98	32	1.0	13.5	16.7	-
50	45°	300	95	35	1.7	24	59	-

Table 1b. Observed liquid level reaches the top endcap (81.8 cm).

Operating point				Estimated values				
V_i/V_e %	β	Q W	T °C	L_p cm	j_g m/s	L_h cm	L_p+L_h cm	L_b cm
50	90°	450	87	52	2.2	30	82	-
50	90°	950	110	52	2.2	30	82	-
100	90°	150	83	-	-	-	-	5
100	90°	250	105	76	0.2	3	79	-

As shown in Table 1, data and estimates are in good agreement and validate the modeling considerations and correlations discussed in the paper for the prediction of the performance of the thermosyphon.

Table 1c. Observed liquid level covers the top endcap permanently.

Operating point				Estimated values				
V_i/V_e %	β	Q W	T °C	L_p cm	j_g m/s	L_h cm	L_p+L_h cm	L_b cm
100	90°	250	37	-	-	-	-	12
100	90°	150	55	-	-	-	-	6
100	90°	200	70	-	-	-	-	5
100	90°	200	83	-	-	-	-	2
100	90°	300	105	80	0.1	2	82	-

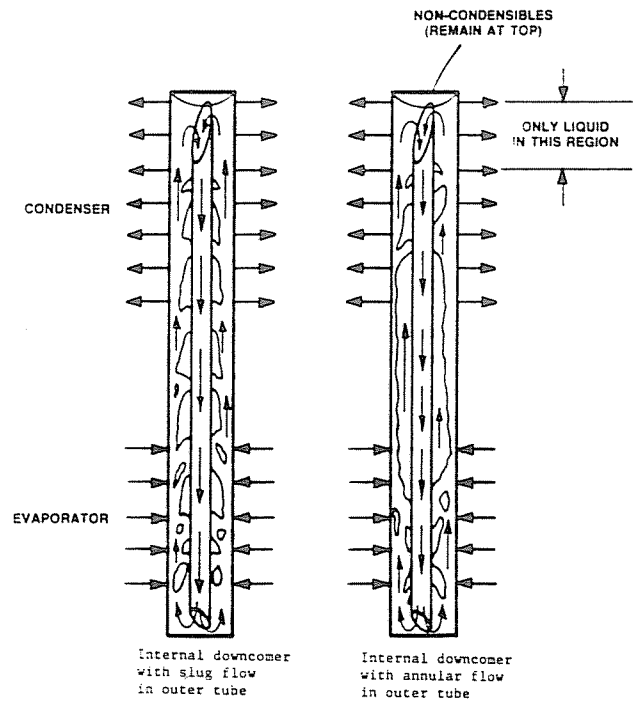

Figure 9. Sketch of the internal downcomer.

DESIGN OF AN INTERNAL DOWNCOMER

With a large enough inventory, the liquid plug that is formed at the top of the thermosyphon allows for the design of an internal downcomer that facilitates a large increase in the operating limit. The highest power throughput reached by the vertical thermosyphon at 98°C (with any inventory) is 1700 W. When a copper tube with internal diameter 4.7 mm and external diameter 6.3 mm is inserted internally to the thermosyphon as sketched in Figure 9 the operating limit at 98°C is 5200 W.

Under the action of gravity the internal downcomer takes the liquid from the plug at the top of the condenser and forces it into the bottom of the evaporator. Operation above the flooding limit is achieved because the liquid return to the evaporator is guaranteed through the downcomer even when the liquid return through the falling film becomes critical. The Nyugen-Chi-Groll correlation (Nguyen-Chi and Groll, 1982) for the flooding limit of a vertical thermosyphon

$$Q = 1.21 \frac{A_x D^{0.5} h_{fg} [\rho_g (\rho_f - \rho_g) g]^{1/2}}{[1 + (\rho_g/\rho_f)^{1/4}]^2} \qquad (17)$$

predicts a flooding limit at 98°C of 2700 W. Figure 9 shows a sketch of the annular flow obtained when operating, with the internal downcomer, above this limit.

CONCLUSIONS

The thermosyphon heat transfer model proposed by Shiraishi, Kikuchi and Yamanishi (1982) has been coupled with the drift-flux model for the estimate of the average liquid level in the thermosyphon at steady-state operation. Experimental data from an apparatus that allows partial flow visualization as well as complete temperature characterization are in good agreement with the model predictions.

The method and results are useful to develop more detailed models of the performance of a closed two-phase thermosyphon. Moreover, operation with an internal downcomer extends beyond the usual operating limits.

ACKNOWLEDGEMENTS

Experimental work entirely supported by a grant from TECOGEN Inc., Waltham, Massachusetts. Additional partial support from the Ministero della Pubblica Istruzione, Roma, Italy.

REFERENCES

Andros, F.E. and Florsehuetz, L.W., 1978, "The Two-Phase Closed Thermosyphon: an Experimental Study with Flow Visualization", in Two-Phase Transport and Reactor Safety, Vol. 4, Hemisphere Pub. Co., Washington, DC, 1231.

Cohen, H. and Bayley, F.J., 1955, "Heat Transfer Problems of Liquid Cooled Gas-Turbine Blades", Proc. Inst. Mech. Eng. (London), Vol. 169, 1063.

Griffith, P., 1964, "The Prediction of Low Quality Boiling Voids", ASME Journal of Heat Transfer, Vol. 83, 327.

Griffith, P., Mohamed, J.A. and Brown, D., 1988, "Dryout Front Modeling for Rod Bundles", to appear in Nuclear Engineering and Design.

Kusuda, H. and Imura, H., 1973, "Boiling Heat Transfer in an Open Thermosyphon", Bulletin of the JSME, Vol. 16, 1734.

Nguyen-Chi, H. and Groll, H.M., 1982, "Entrainment or Flooding Limit in a Closed Two-Phase Thermosyphon", in Advances in Heat Pipe Technology, 4th Intl. Heat Pipe Conf.

Petroff, C., 1988, "The Effect of Liquid Inventory on the Performance of a Closed Two-Phase Thermosyphon", M.S. Thesis, MIT, Cambridge, Mass.

Rohsenow, W.M. and Choi, H., 1961, Heat, Mass and Momentum Transfer, Prentice-Hall, New Jersey.

Shiraishi, M., Kikuchi, K. and Yamanishi, T., 1982, "Investigation of Heat Transfer Characteristics of a Two-Phase Closed Thermosyphon", in Advances in Heat Pipe Technology, 4th Intl. Heat Pipe Conf.

Shoham, O., 1982, "Flow Pattern Transition and Characterization in Gas-Liquid Two-Phase Flow in Inclined Pipes", Ph.D. Thesis, Tel Aviv University, Tel Aviv, Israel.

Wallis, G.B., 1969, One Dimensional Two-Phase Flow, McGraw-Hill, New York.